

Microdisk Lasers

A. F. J. Levi
Department of Electrical Engineering
University of Southern California
Los Angeles, CA 90089-1111, USA

Abstract

InGaAs/InGaAsP quantum well microdisk lasers $0.8\mu\text{m}$ in radius and $0.18\mu\text{m}$ thick with emission at $\lambda = 1.542\mu\text{m}$ can be fabricated and operated at room temperature. Optical mode spacing in such structures is so large that a significant fraction ($\sim 20\%$) of spontaneous emission feeds into the lasing line resulting in superlinear output over a wide pump range.

Introduction

A conventional laser diode consists of an electrically driven semiconductor optical gain medium such as InGaAs placed within a resonant optical cavity. A Fabry Perot cavity, defined by the presence of two parallel mirror faces, results in definite longitudinal optical resonances called cavity modes. Figure 1(a) shows the geometry of such an edge emitting laser. The optically active gain medium is typically $300\text{-}500\ \mu\text{m}$ long, approximately $1\ \mu\text{m}$ wide, and $0.1\ \mu\text{m}$ thick. When electrically pumped, the number of electrons (holes) injected into the conduction (valence) band of a direct band gap semiconductor may be large enough to result in optical gain over a small spectral region near the band edge. Optical gain will approach total optical loss first for the high Q (low loss) Fabry-Perot cavity mode nearest the peak in the gain spectrum. Lasing emission should occur predominantly into this cavity mode because the cavity resonance ensures optical losses are low. However, due to their relatively large size, these devices tend to be power hungry with threshold current for lasing greater than 10 mA. One way to reduce threshold current is to decrease the size of the device and increase the Q of the optical cavity. To some extent the advent of semiconductor microlasers was inspired by such goals.

15 years ago Iga and co-workers at the Tokyo Institute of Technology invented the Vertical Cavity Surface Emitting Laser (VCSEL) [1]. Since then designs have been refined [2] so that today dielectric mirror stacks of the order one micrometer thick above and below a quantum well active region form the high-Q resonant cavity with lasing light emission possible from the surface of the semiconductor substrate. Figure 1(b) shows a schematic diagram of a VCSEL. The optically active gain medium typically consists of one or more approximately 100\AA thick quantum wells placed at an anti-node of the cavity resonance. Small lateral dimensions in the range $3\text{-}20\ \mu\text{m}$ give a potentially superior optical beam profile for launching into optic fiber as well as low threshold currents in the range of 1 mA. Threshold currents would be even lower if more of the optical field were more tightly confined to the gain medium. Never-the-less, while many practical issues still need to be addressed such as the high series resistance for current flowing through the mirror stacks, initial results are encouraging enough that some companies are considering developing VCSEL arrays for use in high speed parallel optical data links.

Recently very small laser diodes have been fabricated using a different type of resonant cavity in which light is very tightly confined to the gain region and emission is in the plane of the semiconductor substrate [3, 4]. The device consists of an InGaAs/InGaAsP multiple quantum well structure formed into a $1.5\text{-}10\ \mu\text{m}$ diameter disk approximately $0.1\ \mu\text{m}$ thick. Electrical current and mechanical support is provided by n- and p-type InP structures above and below the disk. Figure 1(c) shows a schematic diagram of this type of laser and figure 2 shows a scanning electron micrograph of such a microdisk laser. Total internal reflection for photons traveling around the

perimeter of the semiconductor disk result in high Q whispering-gallery resonances. The term "whispering-gallery" is taken from Lord Rayleigh's explanation of sound propagation in the dome of St. Pauls Cathedral, London [5]. In the microdisk laser, the low optical losses associated with high Q whispering-gallery modes allow room temperature lasing action with a measured submilliamp threshold current [4]. Improved designs should result in threshold currents as low as a few tens of microamps. Of course, a consequence of using very high Q resonators is that not much lasing light radiates out into free space. However, it is possible to use light output couplers which slightly spoil the Q and yet allow the emitted light to be increased and redirected in or out of the substrate plane [6]. Other structures which make use of whispering gallery modes, such as the microcylinder laser diode [7], are also being investigated.

Submicron radius disk laser

It is natural to consider how small a microlaser can be made and still function as a laser. In this context it is useful to focus on the microdisk laser since very small gain volumes and high-Q cavities may be simultaneously achieved using this geometry. Figure 3 shows a scanning electron micrograph of a very small optically pumped InGaAs/InGaAsP quantum well microdisk of radius $R = 0.8 \pm 0.05 \mu m$ and thickness $L = 0.18 \mu m$. The disk is composed of six 120 \AA thick quantum wells of InGaAs material lattice matched to InP. Five barriers 120 \AA thick of InGaAsP separate the quantum wells, and InGaAsP layers 240 \AA thick enclose the quantum well-barrier structure. The InGaAsP material has a band-edge corresponding to $1.1 \mu m$ wavelength radiation. After post growth fabrication the device is measured with the sample maintained at room temperature. Optical pump power from a diode laser with emission at wavelength $\lambda = 0.85 \mu m$ is focused onto the disk laser top surface using a 0.5 numerical aperture (N.A.) lens, so that at best only about 80% of total incident pump light is intercepted by the $R = 0.8 \mu m$ radius disk. The total incident pump power, P_{ex} is delivered during an 8 ns period at a repetition period of 100 ns. It is observed that heating becomes significant for pulse widths of 30 ns (30% duty cycle) or greater as evidenced by a decrease of both laser and total light output. The radiation emitted by the microdisk is collected by the same 0.5 N.A. lens, and directed to a spectrometer. The lens collects lasing light scattered by disk imperfections into the vertical direction. The spectra shown in figure 4 were obtained with 5 nm resolution. The figure shows a luminescent background, a lasing line at $\lambda = 1.542 \mu m$, and a resonance at $\lambda = 1.690 \mu m$.

The power in the lasing line versus total incident pump power, P_{ex} , is shown in figure 5. It is clear from this data that output lasing power is superlinear with input. This is in accord with simple models for very small semiconductor lasers and is most readily explained by considering the steady state intensity, S , in the lasing mode. $S = r_{sp}^{mode} / (\kappa - g^{mode})$ where r_{sp}^{mode} is the spontaneous emission rate into the lasing mode, κ is the optical loss rate in the cavity and g^{mode} is the modal gain. For S to reach a given threshold intensity S_{th} when r_{sp}^{mode} is small requires a much smaller value of $(\kappa - g^{mode})$ than when r_{sp}^{mode} is relatively large. Hence, superlinear behavior extends over a larger range of pump power for r_{sp}^{mode} large, because the rate of change in S with P_{ex} around S_{th} is larger when r_{sp}^{mode} is small.

Mode counting

It is possible to construct a straight-forward mode counting argument to calculate the fraction, β , of total spontaneous emission that feeds into the lasing mode. For an ideal disk the whispering mode frequencies ω_M may be calculated to an accuracy of a few percent by solving the equation $2\pi\omega n_{eff}(\omega)R = x_M^1 c$, where c is the speed of light in vacuum, $n_{eff}(\omega)$ is the (two-dimensional)

effective refractive index, and x_M^1 is the smallest positive root of $J_M(x) = 0$, where J_M is the usual Bessel function with integer index M . Larger roots are denoted by x_M^L . The effective refractive index is found from

$$\tan(\pi L \sqrt{\varepsilon - n_{eff}^2} / \lambda) = \sqrt{(n_{eff}^2 - 1) / (\varepsilon - n_{eff}^2)}$$

where ε is the real part of the semiconductor dielectric constant. The small discrepancy between the calculated ($\lambda_5 = 1.480 \mu m$ and $\lambda_4 = 1.634 \mu m$) and experimentally measured ($\lambda_5 = 1.542 \mu m$, $\lambda_4 = 1.690 \mu m$) values of λ_M is in part due to uncertainties in the exact physical dimensions of the disk.

The spontaneous emission rate into a mode may be expressed as

$$r_{sp}^{mode} = \int r_{sp}(\omega) \Gamma(\omega) d\omega$$

where

$$\Gamma(\omega) = \frac{\gamma(\omega) / \pi}{(\omega - \omega_c(\omega))^2 + \gamma(\omega)^2}$$

is the cavity function and $\gamma(\omega)$ describes the frequency dependent line shape of the resonance centered at $\omega_c(\omega)$. For simplicity we consider the case where both ω_c and γ are independent of ω . Clearly, if γ is small, it follows that Γ is a δ -function and so $r_{sp}^{mode} = r_{sp}(\omega_c)$. Even though the cavity line width γ may be small and the spontaneous emission into the mode originates from the frequency interval $\omega_c \pm \gamma$, such emission is enhanced by $1/\gamma$ so that the principle of mode partition is preserved. However, when γ becomes larger than the luminescence width, r_{sp}^{mode} is usually reduced below $r_{sp}(\omega_c)$ by an overlap factor.

Spontaneous emission within a dielectric slab of the disk's thickness ($0.4 \times \lambda$ in the material) and composition is about 75% into trapped transverse electric modes (evanescent above and below the dielectric), 10% transverse magnetic modes and about 15% into free modes propagating outside the dielectric [Ref. 8]. Very little goes into trapped transverse magnetic modes because most of the corresponding modal energies are outside the dielectric. If one assumes these properties of dielectric slabs also apply to disks then about 75% of spontaneous emission is into two-dimensional disk modes of transverse electric character describable by scalar forms $J_M(n_{eff} \omega r / c) e^{iM\theta}$, where θ is the polar coordinate angle and r is the radial coordinate. There are four roots x_M^L of Bessel functions J_M between $x_6^1 = 9.936$ and $x_4^1 = 7.588$, namely $x_5^1 = 8.771$ (corresponding to the $M=5$ whispering-gallery mode lasing emission measured at $\lambda_5 = 1.542 \mu m$), $x_0^3 = 8.654$, $x_2^2 = 8.417$, and $x_3^2 = 9.761$. Thus, in this region, there are about $(2 + 2.5)$ modes in an interval centered on the $M=5$ whispering mode and with endpoints halfway to the adjacent whispering modes. The factor 2.5 is from counting half of the 5 modes corresponding to x_0^3 , x_2^2 , and x_3^2 , taking into account the degeneracy factor of two for $M > 0$. The factor 2 is from x_5^1 and its degeneracy of two. The separation of the $M=4$ and $M=5$ whispering modes is about 150 nm and the measured spectral width of luminescence (full-width-half-maximum) is about 220 nm for $P_{ex} = 1 mW$. Including the 75% factor mentioned above, one may therefore estimate that the fraction of spontaneous emission which goes into one of the $M=5$

whispering gallery modes is $\beta(P_{ex} = 1mW) = (150 \times 0.75) / (220 \times 4.5) = 0.106$, or 0.212 into both $M = 5$ whispering modes.

This result for β appears to be inconsistent with the measured emission shown in figure 4. However, it should be noted that in an ideal disk geometry, radiation from whispering modes is emitted into directions near the plane of the disk, not towards the vertical direction and into the detection apparatus. In addition, the measured smooth luminescence background has a substantial and perhaps dominant contribution from free modes. Furthermore, below transparency, light emitted into whispering modes is substantially absorbed before it escapes the laser structure and is detected. Overall, these effects reduce the apparent β value as determined by casual inspection of the vertically emitted emission spectrum. It is worth mentioning that disk modes other than whispering gallery modes are expected to have relatively low Q values. If a mode width exceeds the luminescence width, the amount of spontaneous emission into such a mode is reduced by an overlap factor. In that case, low Q modes with central frequencies outside the luminescence region experience some spontaneous emission. Never-the-less, the sum of modes times their overlap factor should still give the fraction, β , calculated above.

Device physics

The above results and discussion are representative of present knowledge of microlaser operation. In fact, it is remarkable that, while very small laser diodes have been fabricated, our understanding of how such devices work is manifestly inadequate. Much of what is interesting about microlasers cannot be modeled with the commonly used rate equations for carrier and photon density in the device. In fact, efforts to parameterize microlaser effects with such an unjustifiably simplistic approach are somewhat pointless and bound to fail. The weakness of such modeling motivated the use of mode counting (described above) to establish a value for β . Clearly, it is necessary to examine every relevant aspect of the physics governing device operation before developing a new model for microlasers

The spacing between the mirrors of a standard Fabry-Perot laser is relatively large so that several hundred longitudinal cavity modes overlap the optical gain spectrum. It follows that only a small fraction ($\beta \sim 10^{-4} - 10^{-5}$) of spontaneous photon emission feeds into the longitudinal lasing mode. This combined with the large difference between stimulated and spontaneous recombination rates gives rise to an abrupt increase in lasing light output with increasing drive current above threshold. However, below threshold there is extra photon intensity in cavity modes. In fact, the formal mathematical analogy which exists between a nonequilibrium Landau-Ginzburg phase transition and photon field statistics around threshold allows us to describe all photons in cavity modes below threshold as (unsustainable) fluctuations [Ref 9].

In a very small resonant cavity, such as those used in microcavity lasers, it is possible that only one optical mode overlaps the semiconductor's gain and spontaneous emission spectrum. In such a situation every spontaneous emission event fluctuates into the lasing mode and there is no abrupt increase in average lasing light level with which to define a laser threshold. Similarly, it is no longer possible to define a threshold by considering moments of the statistical distribution in photon number [Ref. 10]. Apparently, the concept of a laser threshold along with the implicitly mean-field language of Landau-Ginzburg phase transitions is no longer useful and a full quantum mechanical description may become necessary [Ref. 11].

It is also worth mentioning that fluctuations in photon number may also be driven directly by fluctuations in electron number. This may become important in microlasers which are so small they operate using only a few thousand electrons. In such a situation the influence of variations in

electron chemical potential can be modified depending on whether the laser is driven by an external voltage or current source.

Of course, the above relates to only one aspect of the problem which, unfortunately, is overshadowed by the more fundamental concern of optical gain in a resonant cavity. Even after several decades of effort, physicists have failed to develop a satisfactory quantitative model of optical absorption and gain in *bulk* intrinsic semiconductors. Such a poor state of affairs is perhaps understandable when one begins to consider the complexity of the problem [Ref. 12]. If one specializes to the case of electron distributions in thermal equilibrium with the semiconductor lattice, then, under low drive current conditions, the semiconductor's band-edge absorption spectrum shows strong conduction/valence band many-electron interaction effects in the form of spectrally sharp exciton features. Under high drive current the semiconductor may contain of order 10^{18} cm^{-3} excess electrons and display optical gain over a small spectral range near the band-edge and absorption elsewhere. Electron interaction effects redistribute and broaden the spectral weight in the exciton features and a significant band tail develops in the semiconductor's renormalized band gap. Even if many-electron interaction effects could be evaluated beyond the mean field (random phase) approximation and a satisfactory quantitative explanation of band tails be established we would still be limited to the case of thermal equilibrium. It seems unlikely, however, that the electron distribution in a microlaser is, in fact, at thermal equilibrium with the semiconductor lattice. The reason for this is that the calculated time scales for various optical and electronic relaxation processes in microlasers are comparable. For example, a microlaser of radius $R = 1 \mu\text{m}$ with emission wavelength $\lambda = 1.5 \mu\text{m}$ has a calculated cavity round trip time of 40 fs, a cavity photon lifetime of 150 fs, and an electron-electron scattering rate in the range of 100 fs. In these circumstances one is tempted to speculate that lasing photons remove electrons from the system at such a fast rate that the electron distribution is unable to equilibrate. The resulting spectral hole burning [Ref. 13] in the electron distribution reduces the spontaneous emission into the lasing mode modifying both the intensity and spectral purity of the microlaser output characteristics. In practice however, except for devices with disk radius less than $1 \mu\text{m}$, this situation is somewhat masked by spatial diffusion of charge carriers from regions of low photon field intensity in the microstructure.

The short and comparable characteristic time scales for cavity round trip time, photon lifetime, and electron-scattering rate in microcavity lasers raises the interesting issue of distinguishing between optical and electronic processes on short time scales. One is tempted to speculate that, since electron scattering is mediated via emission and absorption of a photon, on very short time scales one ultimately cannot distinguish between optical and electronic phenomena.

Conclusion

In summary, room temperature lasing action in a very small InGaAs/InGaAsP quantum well microdisk of radius $R = 0.8 \mu\text{m}$ and thickness $L = 0.18 \mu\text{m}$ has been demonstrated. It is estimated that, for this device, approximately 20% of the spontaneous emission feeds into the $M = 5$ whispering-gallery modes at wavelength $\lambda = 1.542 \mu\text{m}$. Although it should be possible to fabricate even smaller structures which lase into the $M = 4$ whispering-gallery mode, there is still much to be understood about the physics of microlaser operation.

REFERENCES

1. H. Soda, K. Iga, C. Kitahara, and Y. Suematsu, *Japn. J. Appl. Phys.* **18**, 2329 (1979), and K. Iga, S. Kinoshita, and F. Koyama, *Electron. Lett.* **23**, 134 (1987).
2. For a review, see J. L. Jewell, editor of special issue *Microresonator devices*, *Quantum Electronics* **24** (1992).
3. S. L. McCall, A. F. J. Levi, R. E. Slusher, S. J. Pearton, and R. A. Logan, *Appl. Phys. Lett.* **60**, 289 (1992).
4. A. F. J. Levi, R. E. Slusher, S. L. McCall, T. Tanbun-Ek, D. L. Coblenz, and S. J. Pearton, *Electron. Lett.* **28**, 1010 (1992).
5. Lord Rayleigh, *Scientific Papers*, p. 617. Cambridge University, Cambridge, England (1912).
6. A. F. J. Levi, R. E. Slusher, S. L., McCall, J. L., Glass, S. J., Pearton, and R. A. Logan, *Appl. Phys. Lett.* **62**, 561 (1993).
7. A. F. J. Levi, R. E. Slusher, S. L. McCall, S. J. Pearton, and W. S. Hobson, *Appl. Phys. Lett.* **62** 2021 (1993).
8. S. T. Ho, S. L., McCall, and R. E. Slusher, *Quant. Electron. Laser Sci. Tech. Dig.* **11**, 54 (1991).
9. This description is discussed by H. Haken, *Light*, Vol. 2, *Laser Light Dynamics* North Holland, Amsterdam (1986) also see V. DeGiorgio and M. O. Scully *Phys. Rev.* **A2**, 1170 (1970), R. Graham and H. Haken, *Z. Physik* **273**, 31 (1970), S. Grossmann and P. H. Richter, *Z. Physik* **242**, 458 (1971), M. Corti and V. DeGiorgio *Phys. Rev. Lett.* **36**, 1173 (1976).
10. H. J. Charnichael, *Lasers and Quantum Optics*, editors L. M. Narducci, E. J. Quel, and J. R. Tredicce. World Scientific, Singapore (1990).
11. M. Lax, *1966 Brandeis University Summer Institute of Theoretical Physics*, vol. II, editors M. Chretien, E. P. Gross, and S. Deser. Gordon and Breach, New York (1968) also V. Korenman, *Annala of Physics* **39**, 72 (1966).
12. For an overview see *Quantum theory of the optical and electronic properties of semiconductors*, H. Haug and S. W. Koch, World Scientific, Singapore (1990).
13. For a recent discussion on spectral hole burning see K. Henneburger, F. Herzel, S. W. Koch, R. Binder, A. E. Paul, and D. Scott, *Phys. Rev.* **A45**, 1853 (1992).

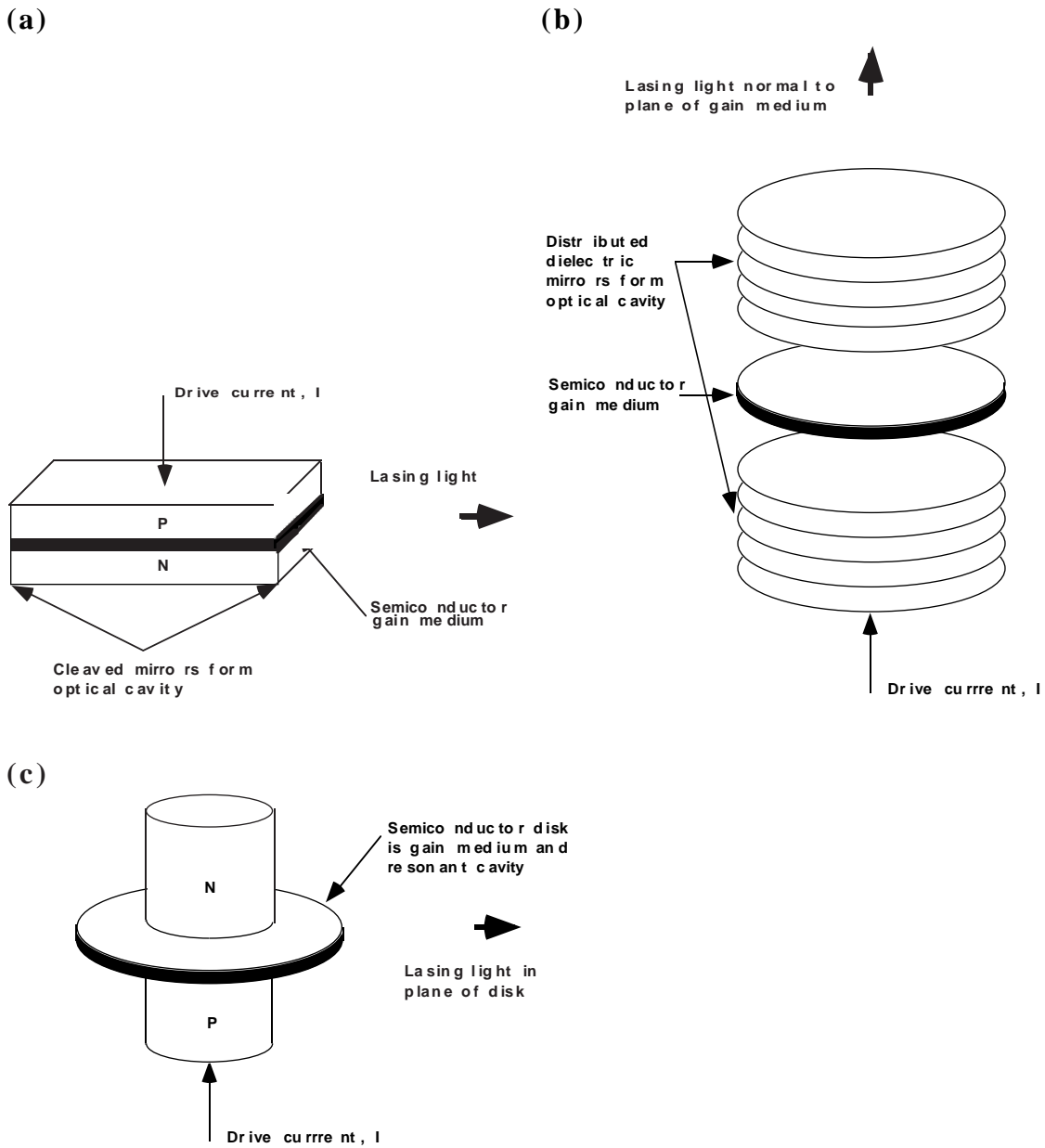


Figure 1 - Schematic diagram of (a) an edge emitting Fabry-Perot laser diode (b) a VCSEL and (c) a microdisk laser. Drive current I is indicated.

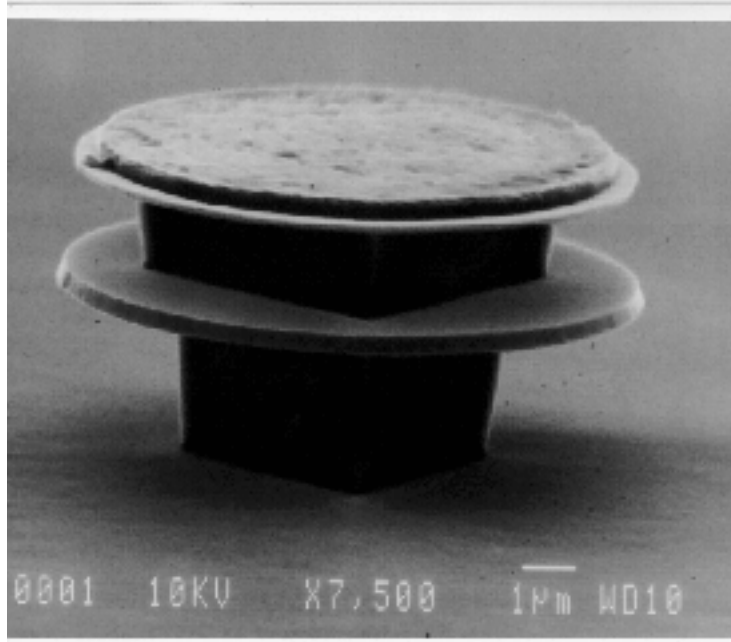


Figure 2 - Scanning electron microscope image of an approximately $10\mu\text{m}$ diameter microdisk laser diode similar to the device discussed in Ref. 4.

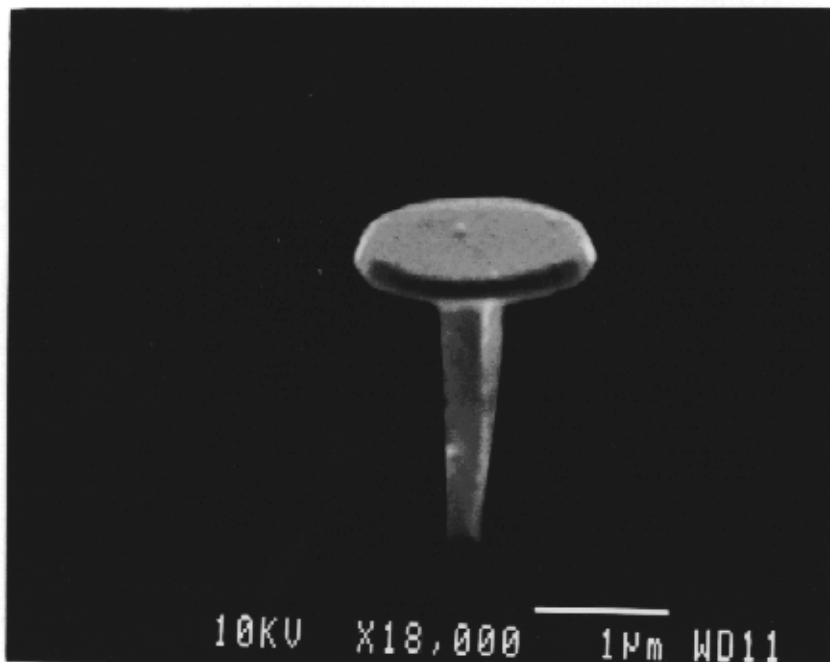


Figure 3 - Scanning electron micrograph of an InGaAs/InGaAsP multiple quantum well microdisk laser with $R = 0.8\mu\text{m}$ and $L = 0.18\mu\text{m}$. The $1\mu\text{m}$ bar provides a scale.

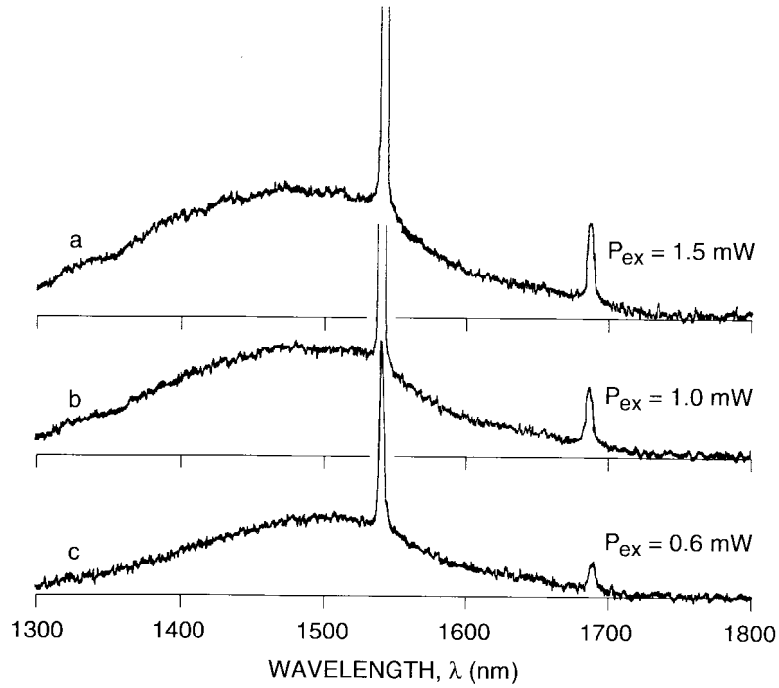


Figure 4 - Room temperature photoluminescence spectra of a $R = 0.8\mu\text{m}$ radius microdisk laser. Excitation is by a pulsed AlGaAs/GaAs laser diode emitting at $\lambda = 0.85\mu\text{m}$. Pump power incident on the device is P_{ex} .

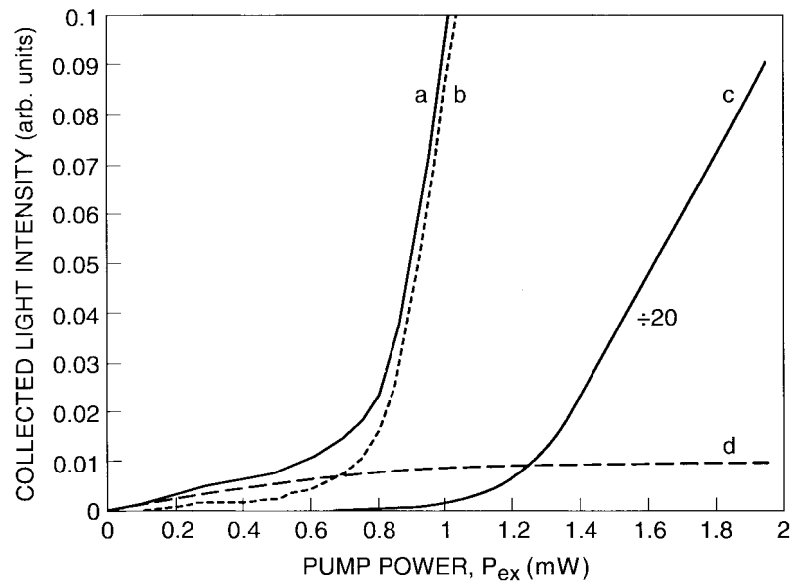


Figure 5 - Room temperature power at the lasing wavelength versus incident pump power, P_{ex} , for the $R = 0.8\mu\text{m}$ microdisk laser of Fig. 3 and 4. (b) Power in the lasing line versus pump power. (c) Power at the lasing wavelength versus pump power. Vertical scale is divided by 20. (d) Power in the spontaneous emission background at the lasing wavelength versus pump power. Resolution is 5 nm.